10. CLIMATE AND THE EQUILIBRIUM STATE OF LAND SURFACE HYDROLOGY PARAMETERIZATIONS

DARA ENTEKHABI and PETER S. EAGLESON

Department of Civil Engineering, Massachusetts Institute of Technology, Cambridge, MA 02139, U.S.A.

Abstract. For given climatic rates of precipitation and potential evaporation, the land surface hydrology parameterizations of atmospheric general circulation models will maintain soil-water storage conditions that balance the moisture input and output. The surface relative soil saturation for such climatic conditions serves as a measure of the land surface parameterization state under a given forcing. The equilibrium value of this variable for alternate parameterizations of land surface hydrology are determined as a fuction of climate and the sensitivity of the surface to shifts and changes in climatic forcing are estimated.

1. Introduction

The storage of heat and moisture in the soil is a key factor in determining the spatial and temporal character of climate; it modulates the diurnal and seasonal periodicities of atmospheric heat and moisture fluxes. Moisture mass added to the soil store is released back to the atmosphere with delays considerably longer than that characteristic of moisture residence in the atmosphere. An interactive soil water reservoir is thus partly responsible for the persistence and long time scales associated with near surface fluctuations in temperature and relative humidity (Delworth and Manabe, 1989). As for the cycle of energy in the atmospheric system, the land surface plays a pivotal role in transforming much of the incident solar energy into heat available for the atmosphere. There is a strong coupling between the moisture and heat stores at the land surface by which the partitioning of heat fluxes into sensible and latent is determined.

In assembling numerical models of climate, it is therefore imperative that the land surface dynamics be properly defined. Otherwise the model climate will fail to reproduce the current state, and the numerical laboratory will be an unreliable device for the study of atmospheric variability and climate change.

One of the main challenges in developing models for the land surface hydrology in numerical climate models stems from the fact that the space-time resolution of these models (10^4 to 10^6 km^2) is incompatible with the characteristic scales of surface hydrologic processes. What cannot be explicitly resolved within the numerical model discretization must be parameterized.

Almost by definition, a parameterization, as opposed to a solution, implies that compromises have been made. In modelling the dynamics of land surface heat and moisture fluxes, the first compromise has been to assume that large land areas respond as uniform hydrologic units; each grid area is assumed to be characterized

Surveys in Geophysics **12**: 205–220, 1991.

by state variables that are representative of all points at the subgrid scale. The surface runoff and evapotranspiration of soil water are then modelled for all points in the area based on the grid average state variable or prognostic.

Expressions for the runoff ratio (ratio of surface runoff to incident precipitation) and the evaporation efficiency (ratio of actual to potential evaporation) used in most operational numerical climate models are simple linear or broken linear functions of the moisture content in the topmost soil layer. These are empirical expressions that have been calibrated to reproduce the long-term and large-scale components of continental water balance for a specific numerical climate model. One example of such an approach to the land surface hydrology parameterization is contained in the NASA Goddard Institute for Space Studies (GISS) General Circulation Model (GCM) (Hansen *et al.* 1983).

The requirement to capture the dynamics of land surface processes in a more realistic manner prompted the development of more detailed parameterizations. These more recent approaches are based chiefly on constructing multiple soil and canopy layers at the land surface. The fluxes of heat and moisture among the layers are then computed based upon the resistance formulation (Dickinson *et al.* 1981) (Sellers *et al.* 1986). For these parameterizations as well, the large numerical grid area is assumed to act as a spatially uniform hydrologic unit. These models are computationally demanding and require extensive data on the resistance parameters for the soil and canopy layers.

As an alternative, Entekhabi and Eagleson (1989) introduced physically-based GCM parameterizations for land surface processes that include the effects of subgrid scale spatial variability in selected key parameters. In Section 2 a brief overview of the runoff ratio and bare soil evaporation efficiency as derived by them is presented. Also included is a summary description of the same functions as they appear in the GISS GCM. This latter land surface parameterization is considered to be typical of the modelling approach used in most current and operational GCMs. It serves as the basis for comparison with the land surface hydrology parameterization of Entekhabi and Eagleson (1989).

Section 3 introduces the concept of water balance under equilibrium conditions (when storage terms disappear). Since the infiltration input (related to the runoff ratio) and the evaporation output are modelled and applied independently, their intersection or equilibrium point reveals the state of the prognostic or state variable soil moisture that is an inherent characteristic of the parameterization.

In the case of land surface hydrology, relative soil saturation is the relevant prognostic and descriptor since it is the key controlling factor that determines the rates of runoff and evaporation. In Section 3, the inherent relative soil saturation at the surface implied by the different soil hydrology parameterizations will be determined as function of climate. Sensitivities of this state of land surface hydrology to shifts and changes in climatic forcing are then estimated. The response of the land surface to marginal changes in forcings for different climate types are also determined.

2. Land Surface Hydrology Parameterizations

Those parameterizations that most control the dynamics of land surface hydrologic processes in climate models are the runoff ratio (R) and the evaporation efficiency (β). Both functions are dimensionless and range between zero and one. Parameterizations for R and β are mostly dependent on the relative soil saturation (s) in the topmost soil layer. This controlling prognostic is the key state variable for soil hydrology and it is basically the ratio of the actual to maximum soil water content in the layer. In the next two subsections, parameterizations for R and β as functions of s will be reviewed briefly for both the Hansen *et al.* (1983) GISS GCM and the Entekhabi and Eagleson (1989) model. Details for the latter parameterization are available in the reference.

a. Surface runoff

Surface runoff in the GISS GCM is generated by removing a fraction R of the rainfall incident at the surface. This fraction is related to the relative soil saturation in the topmost soil layer by

$$R = \varepsilon s. \tag{1}$$

In this way runoff increases with grid surface wetness. For the GISS GCM an ε value of one-half yields continental discharge volumes compatible with observations.

Entekhabi and Eagleson (1989) sought to improve the runoff parameterization by (1) introducing subgrid scale spatial variability over the large GCM grid area, and (2) using a physics-based equation of infiltration. In their parameterization, surface runoff is produced through the independent interaction of two spatially distributed variables: (1) point rainfall intensity (P) over the storm fraction (κ) of the GCM grid, and (2) relative soil saturation, s. Runoff results from both infiltration-excess and partial area (rainfall over impermeable and saturated surfaces) mechanisms as in

point surface runoff =

Infiltration excess ($P - f^*$ for $P > f^*$ and $s < 1$) +

Partial area (P for $s \geq 1$),

where f^* is the infiltration capacity.

Observations of rainstorm mesoscale structures suggest that, within the storm (areal fraction κ), rainfall intensities are exponentially distributed. Using this subgrid description of rainfall and an independent gamma statistical distribution for subgrid point soil moisture values, Entekhabi and Eagleson (1989) derive the closed-form expression for GCM grid runoff ratio as

$$R = 1 - \frac{\gamma\left(\alpha, \dfrac{\alpha}{E[s]}\right)}{\Gamma(\alpha)} + \frac{e^{-\kappa I(1-v)}\,\gamma\left(\alpha, \kappa I v + \dfrac{\alpha}{E[s]}\right)}{\left(\dfrac{\kappa I v E[s]}{\alpha} + 1\right)^{\alpha}\Gamma(\alpha)} \tag{2}$$

where $\gamma(\,,\,)$ and $\Gamma(\,)$ are the incomplete and complete gamma functions, v is a combination soil hydraulic parameter that results from using a physics-based infiltration function, and $E[\,]$ is the spatial expectation operator. Here α is the inverse-square of the dimensionless spatial coefficient of variation (cv) for the statistical distribution of soil moisture at the subgrid scale. Increasing topographic variability within the GCM grid will increase the coefficient of variation due to the effects of lateral soil moisture redistribution on the hillslope. When $cv = 1$, the subgrid statistical distribution is exponential. The dimensionless parameter I in (2) is

$$I = \frac{K_{\text{sat}}}{E[P]}, \tag{3}$$

where K_{sat} is the soil saturated hydraulic conductivity and $E[P]$ is the grid mean rainstorm intensity as produced by the GCM atmospheric computations.

Table I contains typical soil hydraulic properties that are needed to evaluate the runoff ratio. Notice that this parameterization requires only grid-average prognostics for rainfall and soil water content ($E[P]$ and $E[s]$) even though subgrid scale spatial variability is allowed through the statistical distributions. These grid-average prognostics are the same as those used in current GCMs. Thus Equation (2) may be incorporated in land surface parameterizations without significant alterations in GCM computer code.

As illustration, the behavior of R as a function of $E[s]$ and for different storm areal coverages (κ) is presented in Figure 1. As the storm size relative to the GCM grid area decreases (low κ), the runoff that is due to infiltration-excess increases. For low values of κ, the grid mean rainfall is concentrated in a smaller area and will thus achieve greater intensities (i.e. convective rainfall). Entakhabi and Eagleson (1989) present other families of curves for R that illustrate the roles of soil type, spatial variability, the relative contributions of gravity-induced and capillary-induced infiltration and other factors.

b. Bare soil evaporation

The evaporative loss from soil storage is taken to be a fraction β of the potential evaporation (i.e. effectively evaporation under conditions of surface saturation). In

TABLE I

Soil texture and hydraulic properties

Soil texture	Soil composition % (sand, silt, clay)	Porosity	Pore size distribution index m	Saturated hydraulic conductivity $[10^{-3}\ \text{m hr}^{-1}]$
Light	(75, 20, 5)	0.28	2.7	6.08
Medium	(30, 35, 35)	0.36	1.6	3.13
Heavy	(15, 15, 70)	0.41	1.0	1.67

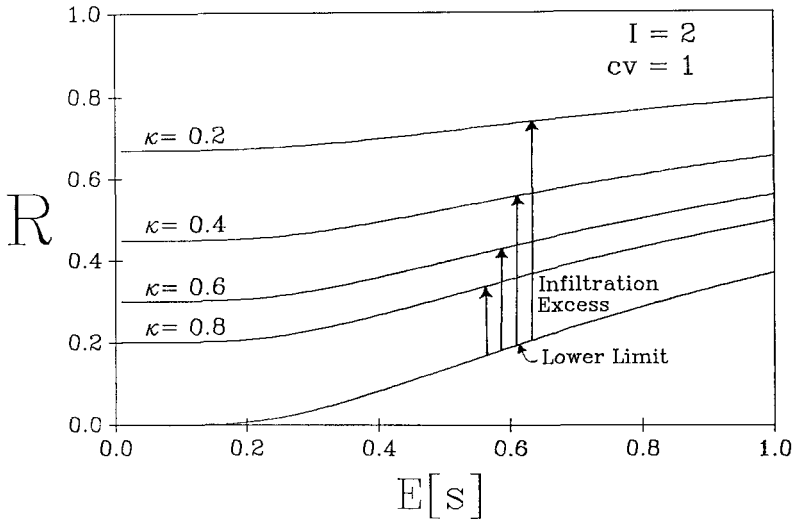

Fig. 1. Runoff ratio R dependence on the grid mean relative soil saturation $E[s]$ for different fractional storm coverage values κ (Entekhabi and Eagleson 1989).

the GISS GCM, Hansen *et al.* (1983) use

$$\beta = s, \tag{4}$$

whereby full evaporation efficiency is not allowed until the soil becomes saturated.

Entekhabi and Eagleson (1989) formulate the parameterization for bare soil β based on subgrid spatial variability in soil saturation and a physics-based exfiltration function. At points within the GCM grid, the evaporation regime may be either climate-controlled or water-limited. In the former regime, the soil potential exfiltration rate exceeds the atmospheric evaporative demand; thus the evaporation rate is limited only by the available energy and it equals the potential rate. In water-limited evaporation regimes, however, the soil media exerts resistance to moisture flux and the local evaporation efficiency fall below unity. The relative soil saturation level s^* at which the transition between the two regimes occurs is a function of soil type and potential evaporation.

Entekhabi and Eagleson (1989) define the dimensionless soil-climate parameter

$$\mathscr{E} = \frac{E[s]}{s^*} \tag{5}$$

and write the bare soil evaporation efficiency for a grid as

$$\beta = 1 - \frac{\gamma(\alpha, \alpha\mathscr{E}^{-1})}{\Gamma(\alpha)} + (\alpha\mathscr{E}^{-1})^{-1/2m-2}\left[\frac{\gamma\left(\frac{1}{2m}+2+\alpha, \alpha\mathscr{E}^{-1}\right)}{\Gamma(\alpha)}\right], \tag{6}$$

where m is the pore-size distribution index for the given soil type as defined in the

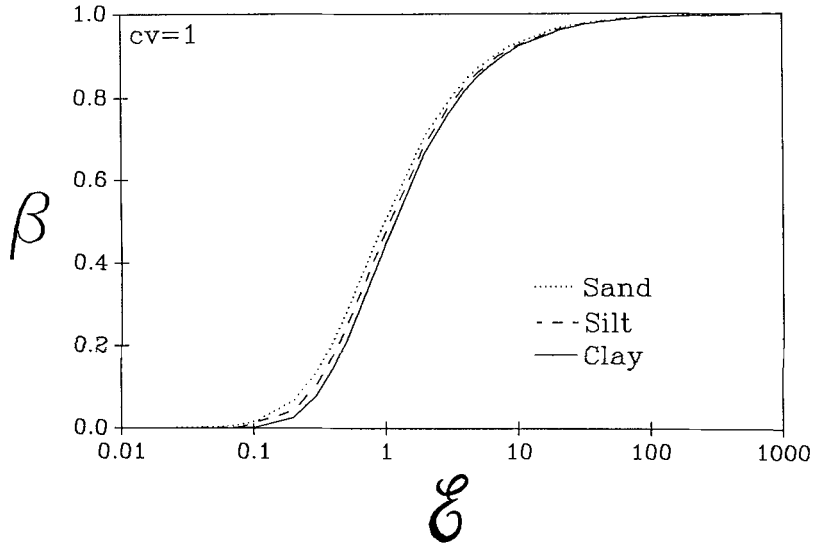

Fig. 2. Bare soil evaporation efficiency β as a function of the dimensionless evaporative regime parameter $\mathscr{E}$ (Entekhabi and Eagleson, 1989).

Brooks-Corey formulation of unsaturated soil hydraulic properties (Eagleson, 1978a). Figure 2 illustrates the dependence of β on $\mathscr{E}$. There is a considerably larger dependence on soil type than that apparent in the Figure since $\mathscr{E}$ itself is a strong function of soil type. Entekhabi and Eagleson (1989) present figures illustrating the relation between s^* and potential evaporation for different soil types, the relative roles of gravity and capillarity in the bare soil evaporation process and the role of spatial variability on β. On the last point, it should be clear that with low amounts of subgrid scale spatial variability in soil moisture, the evaporation efficiency is near unity for $E[s] \geqslant s^*$ or $\mathscr{E} \geqslant 1$ and is rather small for $\mathscr{E} < 1$. Thus for small cv, β aproaches a Heaviside function with transition at $\mathscr{E}$ near unity.

3. Equilibrium State of Land Surface Hydrology

The water balance at the land surface is

$$\frac{dw}{dt} + Q = P - e, \tag{7}$$

where w is the soil water storage depth and Q, P, and e are the runoff, precipitation, and evaporation rates respectively. At equilibrium, we may write the climate water balance as

$$Q = P - e. \tag{8}$$

In Section 2, the runoff rate Q is defined as the fraction R of precipitation and the evaporation rate e is taken to be the proportion β of the potential evaporation

rate e_P. Upon substitution of these definitions,

$$RP = P - \beta e_P$$

or

$$\Upsilon = \frac{\beta}{1 - R} \tag{9}$$

where

$$\Upsilon = \frac{P}{e_P} \tag{10}$$

Parameter Υ is a dimensionless measure of climate.

Arid regions are characterized by Υ approaching zero but humid regions may achieve Υ values of up to 2.

The right-hand side of (9) involves only the runoff ratio and the evaporation efficiency. These functions are defined chiefly through the surface relative soil saturation s which is the key soil state variable in such parameterizations of land surface hydrology. Thus from (9), and for a given climate Υ, there must exist an equilibrium value of soil moisture which will evaluate R and β to correspond to the climate. It is such values of soil moisture that interest us here. This is analogous to the analysis used by Eagleson (1978b) in order to evaluate runoff yield based on regional climate information.

Given a specific parameterization for R and β, there will be different equilibrium relative soil saturation solutions over the range of climate Υ, i.e. $s = s(\Upsilon)$. This state can be clearly demonstrated for the GISS GCM soil hydrology. With (1) and (4), (9) becomes

$$\Upsilon = \frac{s}{1 - \varepsilon s}$$

or

$$s = \frac{\Upsilon}{1 + \varepsilon \Upsilon} \tag{11}$$

Such a simple solution is possible in this case since the GISS GCM soil hydrology parameterization for R and β are linear functions of soil moisture alone.

In the case of the Entekhabi and Eagleson (1989) subgrid parameterization, the runoff ratio and the evaporation efficiency are highly nonlinear functions of the relative soil saturation. These functions furthermore depend on storm intensity, soil type and degree of spatial variability.

In the case of the subgrid runoff parameterization for R, take the variable I (Equation (3)) as the ratio of the saturated hydraulic conductivity and the climatic precipitation rate. In estimating infiltration-excess runoff, it is necessary to scale the value of I to represent storm intensities. Values of I are multiplied by $\kappa\lambda$; where κ

is the fractional spatial storm coverage as before and λ is an analogous temporal probability of rainfall.

The subgrid parameterization for the bare soil evaporation efficiency β is chiefly dependent on the dimensionless evaporative regime parameter $\mathscr{E}$. For a given climate Υ, $\mathscr{E}$ may be written as

$$\mathscr{E} = (\Upsilon I \Omega)^{2m/(1+4m)} \tag{12}$$

where I is linked to the runoff parameterization and Ω is a dimensionless soil type parameter (see Entekhabi and Eagleson (1989) for details).

a. GOVERNING SOIL MOISTURE CONDITIONS

For given climates and soils (i.e. given Υ, I, and soil hydraulic properties), (9) may be solved for the equilibrium relative soil saturation when β and R are defined with the Entekhabi and Eagleson (1989) subgrid parameterization.

Figure 3 illustrates the equilibrium relative soil saturation (s) for different climates (Υ) in the cases of the simple soil hydrology and the subgrid model. The Entekhabi and Eagleson (1989) subgrid model equilibrium soil saturation is determined numerically for $cv = 1$ (i.e. exponential soil moisture spatial distribution) and a medium soil type. Table I contains the definition of soil types and furthermore lists the hydraulic properties for various soil textures.

In general terms, both the GISS soil hydrology and the subgrid parameterization yield similar functional dependencies between the soil hydrology moisture content state variable and climate. There are, however, several points of departure which reveal facts about the nature of each parameterization.

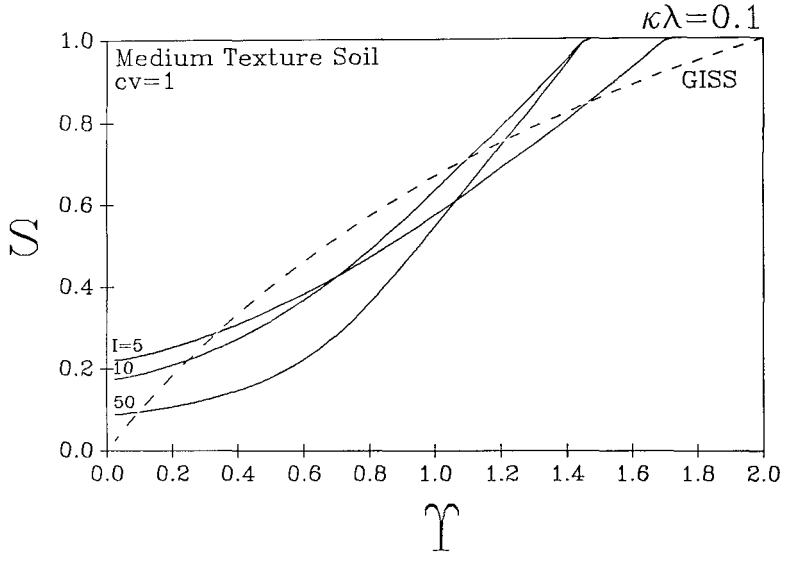

Fig. 3. Equilibrium relative soil saturation for the Entekhabi and Eagleson (1989) subgrid model with medium texture soil and $cv = 1$ and for the GISS GCM soil hydrology.

In the case of the GISS soil hydrology, the parameter ε determines the shape and upper Υ-limit of s. For low values of ε, the parameterization will yield linear dependence between s and Υ. For successively larger values of ε, the approach to the limit is delayed until high Υ (humid climates).

The subgrid parameterization yields saturated surfaces for Υ between 1.3 and 1.7 in this case (Figure 3). Over the range of Υ, the subgrid hydrology gives lower equilibrium relative soil saturation values when compared to the GISS GCM soil hydrology except at the aforementioned high Υ limit and the low Υ end where there exists a lower limit to surface dryness for all climates. Thus the soil hydrology is not as sensitive at this low end of the Υ scale to changes in Υ. This feature of the subgrid model helps in maintaining a minimum moisture content in the soil under arid conditions.

In order to illustrate the utility of the curves in Figure 3, comparisons are made between the equilibrium solution defined here and those obtained from computer simulation with a numerical climate model. Figure 4 represents the experimental (via lengthy numerical simulations) values of the equilibrium relative soil saturation plotted versus climate Υ. Computer simulations are performed with the Entakhabi (1990) climate model which includes GCM physical modules such as land surface hydrology, radiative transfer, moist convection and other essential parameterizations. The set of 15 numerical experiments (each represented by circle symbols in Figure 4) were performed using the subgrid hydrology with medium soil, $cv = 1$ and $\kappa = 0.6$. In order to compare the simulation results with the equilibrium soil moisture variable derived simply from Equation (9), we superpose the curve of equilibrium

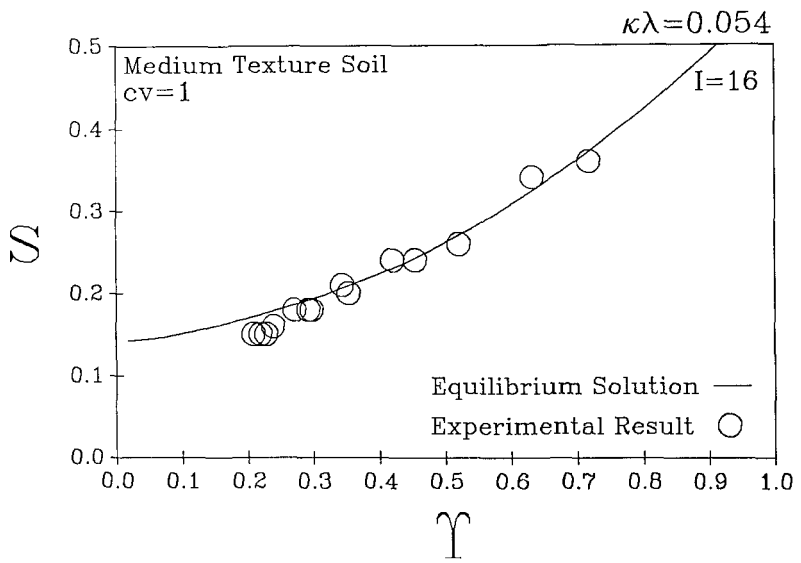

Fig. 4. Relative soil saturation versus climate parameter Υ for numerical experiments with the Entekhabi (1990) numerical climate model and for the equilibrium solution of the subgrid model.

relative soil saturation for the relevant value of I (as in Figure 3). The 15 experimental points have a mean precipitation rate of 4.8 mm day^{-1}. The temporal probability of rainfall for these simulations averages 0.09 (value for λ); a low value since the model is mostly convectively driven. Given the medium textured soil saturated hydraulic conductivity (Table I), the population I value is thus 16. With $\kappa = 0.6$ for the simulations, we obtain $\kappa\lambda = 0.054$. The comparison between the computer simulation results and the simpler method of inverting Equation (9) for relative soil saturation is favorable. The departures are contributed to the approximations made in finding common values of $\kappa\lambda$ and I for all 15 simulations.

Notice that the experimental values in Figure 4 required considerable computer resources and involved a numerical climate model. Moreover they cover only a small region of the Υ scale. The much simpler procedure of solving Equation (8) for relative soil saturation yields similar but more general results with much less effort. Furthermore, the simpler approach allows us to test the sensitivity of the parameterization to soil type and spatial variability.

Using the equilibrium soil saturations derived in Figure 3, we evaluate the evaporation efficiency β for different climates Υ. Figure 5 illustrates this case by relating Υ and the subgrid climate value for β. Also plotted is the L'vovich (1979) equivalent formulation that is a fit to observations. The subgrid curve and the L'vovich formula correspond well, especially for low values of Υ. At higher Υ, the subgrid curves terminate when the soil is completely saturated.

Using the simple procedure established for determining the equilibrium relative soil saturation as a function of climate, we now proceed to perform some basic

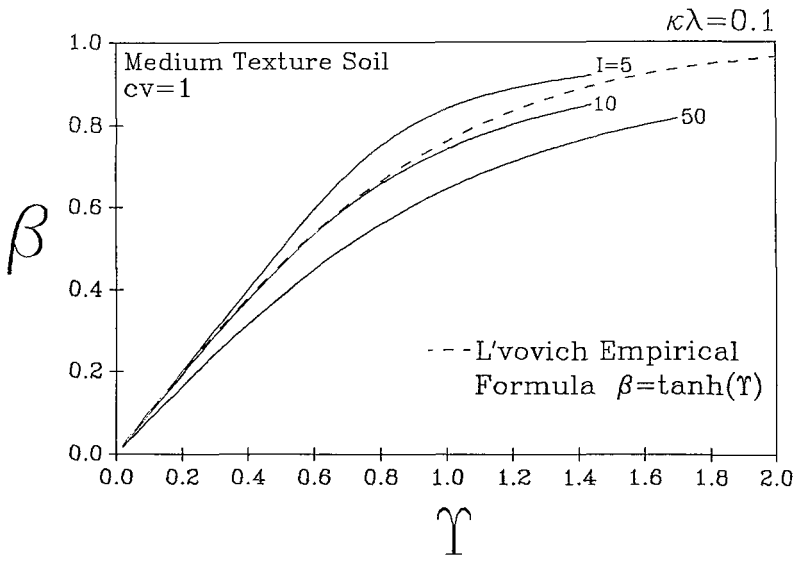

Fig. 5. The evaporation efficiency β function of different climate Υ for the subgrid model compared to the L'vovich (1979) empirical forumla.

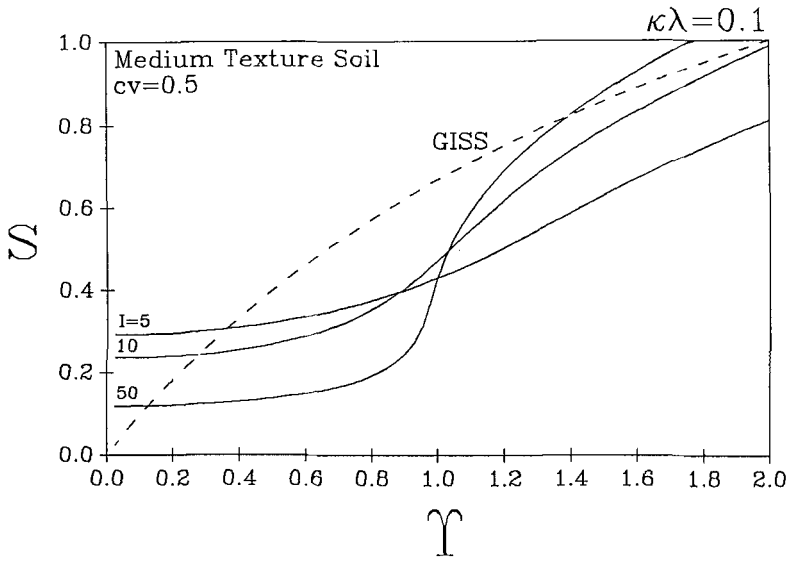

Fig. 6. Equilibrium relative soil saturation for the subgrid model with medium textured soil and $cv = 1/2$ and for the GISS GCM soil hydrology.

sensitivity tests. Figure 6 illustrates the equivalent results of Figure 3 but now for $cv = 1/2$. Reduced spatial variability of surface soil moisture results in the sharp change in behavior of soil hydrology around the point when the land surface shifts from the water-limited to the climate-controlled evaporative regime (just below $\Upsilon = 1$). The evaporation efficiency function for low spatial variability behaves similarly to a Heaviside function with an analogous transition point. The lower limit to soil saturation and an extended range of Υ over which the soil will remain less than saturated is evident in Figure 6.

Figure 7 demonstrates the role of soil texture in the determination of the equilibrium relative soil saturation for different climates. Using the definitions of soil type in Table I, and for a similar total soil depth, it is evident that heavier textured soils attain lower equilibrium moisture levels for more arid climates (low Υ). This behavior is attributed to the greater desorptive property of these soils. Moreover, these low hydraulic conductivity soils have greater surface runoff loss. In more humid climates, the light textured soils have the lesser equilibrium relative soil saturation.

b. SENSITIVITY TO CLIMATIC FORCING

Now that the equilibrium relative soil saturation (s) and climate (Υ) are related in a simple manner, i.e. $s = s(\Upsilon)$, we can proceed to define more direct measures of sensitivity. The sensitivity of this chief state variable in soil hydrology to variability and climatic change in Υ may be formulated in terms of the elasticity of s with

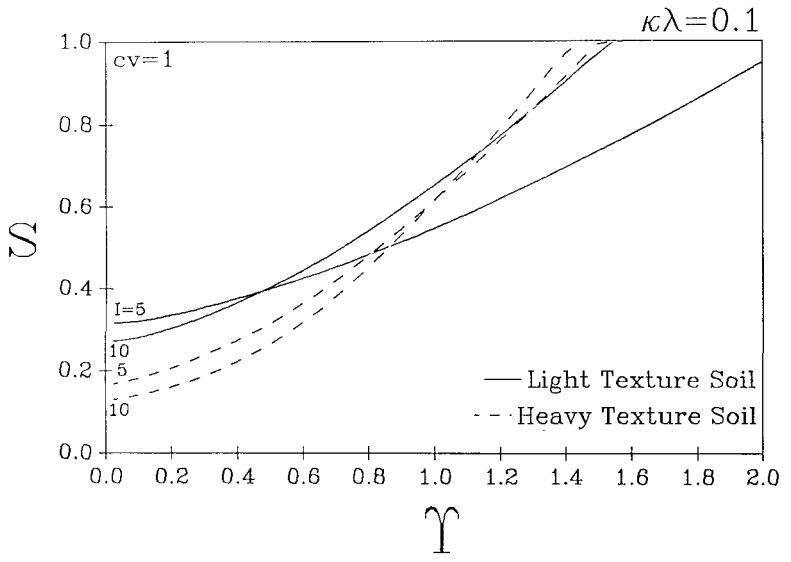

Fig. 7. Equilibrium relative soil saturation for the subgrid model with light and heavy textured soils and $cv = 1$.

respect to Υ. This measure is common in microeconomics where the relative response of, say, demand to changes or perturbations in price is determined. Elasticity is defined as the dimensionless

$$\frac{\Upsilon}{s}\frac{\partial s}{\partial \Upsilon}. \tag{13}$$

This number represents percent change in relative soil saturation due to percentage change in climate parameter Υ. This measure of soil moisture elasticity is different for the diverse climate types (Υ).

Figures 8, 9, and 10 illustrate the elasticity measure for the cases presented in Figures 3, 6, and 7. With medium textured soil and $cv = 1$ (Figure 8), the lower limit to soil moisture evident in Figure 3 is reflected as low elasticity at small Υ values. The GISS GCM soil hydrology, however, has its greatest sensitivity to climatic shifts at this arid end of the climate scale (near one-to-one correspondence). The subgrid model, however, is sensitive to climatic perturbations and change for climates that are at the margin of transition between the water-limited and climate-controlled evaporative regimes.

The subgrid parameterization higher sensitivity at this climate margin is more clearly evident for the reduced spatial variability case ($cv = 1/2$; Figure 9). With less spatial variability over the large land area, the transition between the two evaporative regimes is even sharper; here the evaporation efficiency β approaches the Heaviside function. Thus at the margin of the two climate regimes, the land surface sensitivity to climatic shifts in Υ as defined through elasticity is greatest (Figure 9).

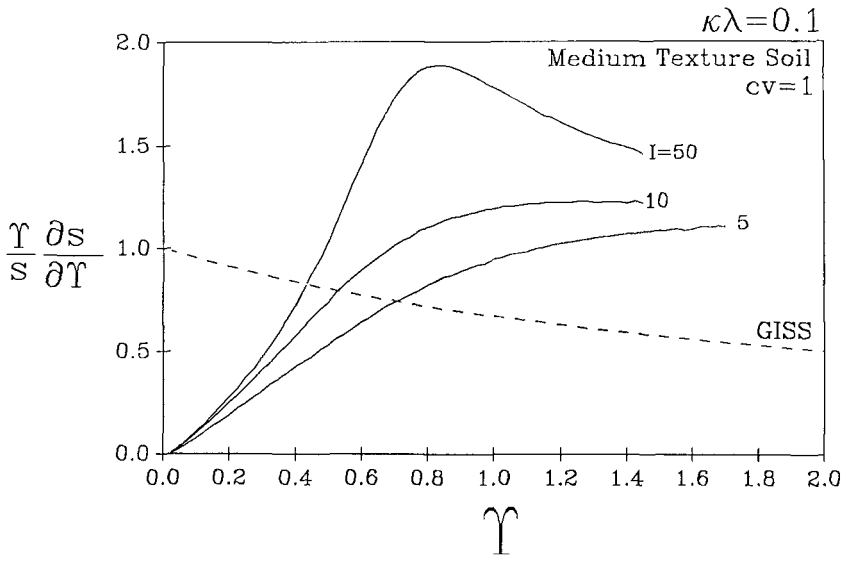

Fig. 8. Soil moisture elasticity with respect to the climate parameter Υ for the GISS GCM soil hydrology model and the subgrid model with medium textured soil and $cv = 1$.

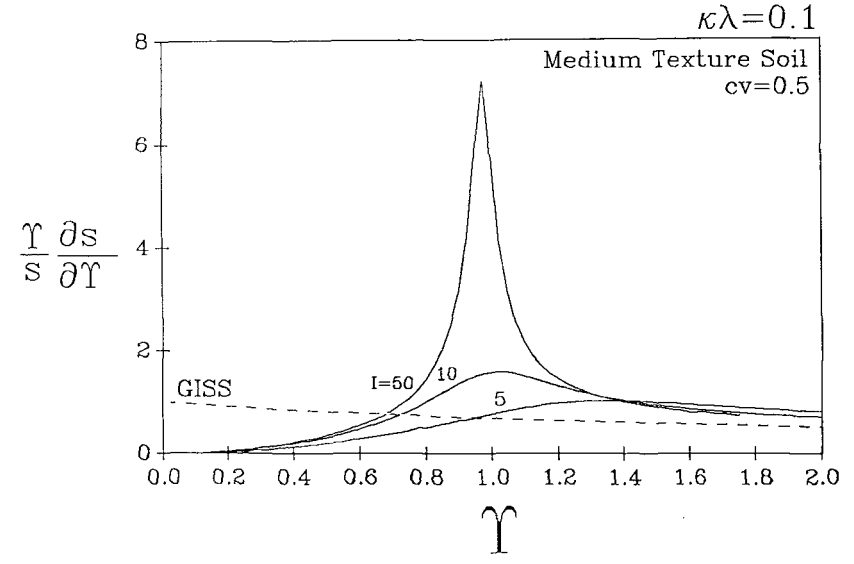

Fig. 9. Soil moisture elasticity with respect to the climate parameter Υ for the GISS GCM soil hydrology model and the subgrid model with medium textured soil and $cv = \frac{1}{2}$.

The role of soil type is illustrated through Figure 10. Here the relative soil saturation elasticity with respect to climate Υ is represented for both the light and heavy textured soils. Over the entire range of climate types, the heavy textured soil with large clay and silt fractions exhibits greater sensitivity to perturbations and shifts in climate.

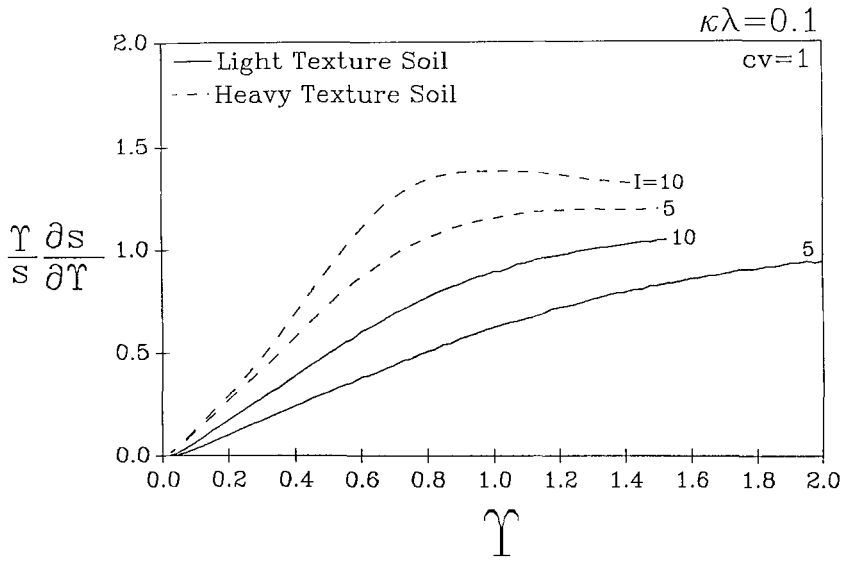

Fig. 10. Soil moisture elasticity with respect to the climate parameter Υ for the subgrid model with $cv = 1$ and light and heavy textured soils.

4. Summary

The equilibrium soil moisture content, normalized by its saturation value, is functionally related to a dimensionless measure of climatic forcing Υ (ratio of rainfall to potential evaporation). For two alternative parameterization of land surface hydrology (Hansen *et al.* (1983) GISS GCM soil hydrology and the Entekhabi and Eagleson (1989) parameterization that includes subgrid scale spatial variability), the equilibrium soil moisture for the range of Υ are evaluated. In the case of the parameterization that incorporates the effects of subgrid scale spatial variability and soil physics, comparisons are made in order to determine the response of the soil moisture state variable to spatial variability and soil type.

The land surface hydrology undergoes a sharp change in behavior at the limit where a transition occurs between water-limited and climate-controlled evaporative regimes. Increased spatial variability over the land surface results in the broadening of the interval over which the two evaporative regimes may coexist and thus restrains any abrupt shift in soil moisture state variable in response to Υ changes. For similar Υ, soils with higher clay fractions result in lower equilibrium relative soil saturation when compared with their lighter textured sandy soil counterparts since they are characterized by greater desorptive potential during bare soil evaporation. The heavier textured soils also lose a greater fraction of the incident rainfall to runoff due to their low hydraulic conductivity.

The importance of identifying the equilibrium soil moisture as a function of climate for each parameterization lies in the fact that this governing state strongly

influences the heat and moisture climatology of the numerical model. The equilibrium state as implied by the construct of these parameterizations produces a strong field of attraction toward which the numerical climate model is driven. An understanding of this state is thus necessary for the study of the role played by land surface hydrology parameterizations in numerical climate models.

The response of the land surface state to shifts in climatic forcing are quantitatively determined using the soil moisture elasticity function with respect to climatic Υ. The sensitivity is greatest at the transition between the water-limited and climate-controlled evaporative regimes. Neglecting subgrid scale spatial variability further compounds this sensitivity.

Acknowledgements

This work has been supported by the National Aeronautics and Space Administration Grant NAG 5-743.

List of Variables

cv Coefficient of variation in the subgrid spatial distribution of soil moisture [ ]
e Evaporation rate [L/T]
e_P Potential evaporation rate [L/T]
$\mathscr{E}$ Dimensionless soil-climate parameter (Ratio of mean soil saturation to soil saturation at transition between water-limited and climate-controlled evaporative regimes; see Entekhabi and Eagleson (1989); Equation (30)) [ ]
$E[\ ]$ Spatial expectation operator
f^* Infiltration capacity [L/T]
K_{sat} Saturated soil hydraulic conductivity [L/T]
m Pore-size distribution index in the Brooks-Corey parameterization (see Eagleson (1978a)) [ ]
P Precipitation rate [L/T]
Q Surface runoff rate [L/T]
R Runoff ratio (ratio of surface runoff and incident rainfall) [ ]
s Relative soil saturation (Soil moisture content with the residual immobile content removed and normalized by its saturation value) [ ]
s^* Relative soil saturation at the transition between water-limited and climate-controlled evaporative regimes (see Entekhabi and Eagleson (1989); Equations (29) and (30)) [ ]
t Time [T]
v Dimensionless soil parameter measuring the strength of soil capillarity (see Entekhabi and Eagleson (1989); Equation (13)) [ ]
w Soil water depth in storage [L]
α Inverse-squared cv [ ]
β Evaporation efficiency (Ratio of actual to potential evaporation) [ ]
ε Empirical parameter in Equation (1) [ ]
$\gamma(\ ,\ )$ Incomplete gamma function
$\Gamma(\ )$ Complete gamma function
κ Fractional spatial coverage of storms [ ]
λ Fraction of time with rainfall [ ]
Ω Dimensionless soil parameter (see Entekhabi and Eagleson (1989); Equation (30)) [ ]
Υ Ratio of precipitation to potential evaporation [ ]

References

Delworth, T. and Manabe, S.: 1989, 'The Influence of Soil Wetness on Near-Surface Atmospheric Variability', *J. of Climate* **2**(12), 1447–1462.

Eagleson, P. S.: 1978a, 'Climate, Soil, and Vegetation 3. A Simplified Model of Soil Moisture Movement in the Liquid Phase', *Water Resour. Res.* **14**(5), 722–730.

Eagleson, P. S.: 1978b, 'Climate, Soil, and Vegetation 7. A Derived Distribution of Annual Water Yield', *Water Resour. Res.* **14**(5), 765–776.

Entekhabi, D.: 1990, 'A Screening Model for Land Surface Hydrology Parameterizations in Atmospheric General Circulation Models', 59 pp. (to be submitted).

Entekhabi, D. and Eagleson P. S.: 1989, 'Land Surface Hydrology Parameterization for Atmospheric General Circulation Models Including Subgrid Scale Spatial Variability', *J. of Climate* **2**(8), 816–831.

Hansen, J., Russel, G., Rind, D., Stone, P., Lacis, A., Lebedeff, S., Ruedy, R. and Travis, L.: 1983, 'Efficient Three-Dimensional Global Models for Climate Studies: Models I and II', *Mon. Wea. Rev.* **111**(4), 609–662.

L'vovich, M. I.: 1979, *World Water Resources and their Future*, translated by L. Nace, American Geophysical Union, 415 pp.